Electrical Characteristics of Rat Skeletal Muscle in Immaturity, Adulthood and After Sciatic Nerve Injury, and Their Relation to Muscle Fiber Size

Published in final edited form as:
Physiol Meas. 2009 December ; 30(12): 1415. doi:10.1088/0967-3334/30/12/009.

Electrical characteristics of rat skeletal muscle in immaturity, adulthood, and after sciatic nerve injury and their relation to muscle fiber size

Mohammed Ahad, PhD, **P. Michelle Fogerson, BS**, **Glenn Rosen, PhD**, **Pushpa Narayanaswami, MD**, and **Seward B. Rutkove, MD**
Department of Neurology, Division of Neuromuscular Diseases, Harvard Medical School, Beth Israel Deaconess Medical Center, 330 Brookline Avenue, Boston, MA 02215, USA

Abstract

Localized impedance methods can provide useful approaches for assessing neuromuscular disease. The mechanism of these impedance changes remains, however, uncertain. In order to begin to understand the relation of muscle pathology to surface impedance values, 8 immature rats, 12 mature rats, and 8 mature rats that had undergone sciatic crush were killed. Tissue from the gastrocnemius muscle from each animal was measured in an impedance cell, and the conductivity and relative permittivity of the tissue calculated in both the longitudinal and transverse directions for frequencies of 2 kHz to 1 MHz. In addition, quantitative histological analysis was performed on the tissue. Significant elevations in transverse conductivity and transverse relative permittivity were found with animal growth, but longitudinal values showed no difference. After sciatic crush, both transverse and longitudinal conductivity increased significantly, with no change in the relative permittivity in either direction. The frequency dependence of the values also changed after nerve injury. In the healthy animals, there was a strong linear relation between measured conductivity and relative permittivity with cell area, but not for the sciatic crush animals. These results provide a first step toward developing a comprehensive understanding of how the electrical properties of muscle alter in neuromuscular disease states.

Keywords

muscle; electrical impedance; conductivity; permittivity; dielectric

I. INTRODUCTION

Electrical impedance myography (EIM) is an electrophysiologic technique for the assessment of muscle that depends upon the surface application of high frequency electrical current to muscles and the measurement of subsequent voltage patterns (Rutkove *et al* 2002; Rutkove 2009). Although still under refinement, the technique offers the promise of a useful, non-invasive means for the evaluation of neuromuscular disease and to date, we have identified changes in the major EIM parameters, the resistance, reactance, and phase in a variety of disease states (Rutkove *et al* 2005; Tarulli *et al* 2005; Rutkove *et al* 2007). In addition, we have also observed that certain impedance patterns are more predictive of neurogenic disease and others more predictive of myopathic disease (Garmirian *et al* 2009).

Please address correspondence to: Seward B. Rutkove, MD, Beth Israel Deaconess Medical Center, Department of Neurology330 Brookline Avenue, Shapiro 810 Boston, MA 02215; srutkove@bidmc.harvard.edu; Tel: 617-667-8130; Fax: 617-667-8747.

Physics and Astronomy Classification Scheme: 87.19.Ff, 87.19.La, 87.19.Nn

For the most part, our research has focused on performing measurements predominantly in patients, correlating EIM changes to clinical parameters (Tarulli *et al* 2005; Rutkove *et al* 2007). Recently, however, we have initiated a program of reverse translational research, applying EIM to rat models of neuromuscular disease in order to assist in better identifying the mechanistic underpinnings of the observed changes in humans (Nie *et al* 2006; Ahad and Rutkove 2009). We have been able to establish that highly stable EIM data can be acquired from rats by the time they reach about 14 weeks of age and that EIM is sensitive to changes produced by sciatic nerve crush (Ahad and Rutkove 2009).

One major advantage of performing animal studies is that we can kill the animals and evaluate the muscle histologically in order to determine how changes in muscle structure and composition after injury contributes to measured surface EIM data. Equally important, by obtaining actual muscle tissue, we are also able to assess the actual electrical properties—the muscle's inherent electrical conductivity and its permittivity (Epstein and Foster 1983). Ultimately, by connecting these values to the surface measurements *via* the use of finite element analysis, it will be possible to model the changes observed in the rats. In this study, we report our initial efforts in that direction as we measure the electrical properties of rat gastrocnemius muscle in healthy immature and mature animals and in adult animals after sciatic crush and then relate these findings to quantified histological measures.

2. METHODS

2.1 Rats

Given the potential value of this research in the diagnosis and treatment of a variety of human neuromuscular conditions, this animal work was approved by the Institutional Animal Care and Use Committee of the Beth Israel Deaconess Medical Center, Boston, MA. A total of 28 rats were studied: 8 immature rats (weighing 140–160 grams), 20 mature rats (weighing 420–480 gms), of which 8 underwent sciatic nerve crush. All were male Wistar Rats obtained from Charles River Laboratories, Wilmington, MA and were acclimated for 48 hours after arrival at our animal facility before any measurements were obtained. Animals were fed Harlan Teklad Rodent Diet #7964. In the 8 sciatic crush animals, an incision was made proximally in the thigh and the sciatic nerve exposed, being careful not to disturb surrounding tissues, with the animal anesthetized under isoflurane. A 1mm length segment of nerve was then crushed using a jeweler's forceps by applying 3–4 MPa pressure for approximately 30 seconds. The incision was then sutured closed and the animals allowed to recover until they were killed one to two weeks later. Buprenorphine was administered at a dose of 0.5 mg/kg every 24 hours for 2 days after surgery *via* intraperitoneal injection to control pain.

2.2 Needle Electromyography

Limited needle electromyography (EMG) of the lateral gastrocnemius to assess for the presence of fibrillation potentials was performed after to confirm sufficient nerve injury had been achieved. A TECA Synergy T2 EMG Monitoring System (Viasys, Madison, WI) was used for recording *via* a standard concentric EMG needle.

2.3 Impedance Measurement System

A lock in amplifier, Signal Recovery Model 7280, Advanced Measurement Technology Inc., Oak Ridge, TN was used to supply AC currents from its 1V reference output oscillator and the selected voltage was fed to its input terminal through a high impedance and very low capacitance active probe (Model 1103 of Tektronix, Beaverton, OR) as previously described (Esper *et al* 2006). Instrument-interfacing software was written in Visual Basic to calculate resistance and reactance and also display and store recorded impedance data. The system was calibrated with resistor-capacitor circuits of known character, designed to mimic to the

electrical properties of muscle; in addition, the system was also tested using 0.9%, 0.45%, 0.225% and 0.1125% saline solutions to confirm data consistency.

2.4 Measurements of the electrical constants

After obtaining surface impedance measurements over the gastrocnemius muscle (a foot flexor), as reported in Ahad and Rutkove 2009, and with the animals still under anesthesia, the skin overlying the leg was cut with a scissors and the tissue dissected down to expose the entire gastrocnemius muscle. The animal was then killed *via* an overdose of intraperitoneal Nembutal® or FatalPlus® and the entire gastrocnemius muscle immediately excised at its proximal extent just below the knee and distally by cutting the gastrocnemius tendon at its insertion into the calcaneus. A superficial portion of this muscle, approximately 1cm × 1cm square of about 0.4cm height was excised with a scalpel. The tissue was kept moist and warm by its being covered with 0.9% saline-saturated gauze under a heating lamp, maintaining the tissue at 36–7°C. All animals were killed between days 7 and 14 after crush, with one to two being studied per day.

This tissue was then placed into a 1cm × 1cm × 2cm plastic measuring cell between two stainless steel current electrodes with the fiber orientation perpendicular to the metal electrodes (providing longitudinal measurements), similar to the approach of Baumann et al (Baumann *et al* 1997). The top cell was fitted with a removable plastic lid with four holes, each 2mm apart from each other and with the outermost holes also 2mm away from the edge of the cell. The current electrodes were 1cm in width and 5 cm in length, and thus contacted entirely the two sides of the rectangular slab of muscle. Two disposable monopolar EMG needle electrodes of Viasys Healthcare (Ref# 902-DMG50) were used as two voltage-measuring electrodes. These two voltage electrodes were inserted through the holes of the plastic cover such that they just contacted the surface of the muscle without inserting them, and measurements were made using the above system in the 2 kHz to 1MHz range. The muscle was then rotated 90 degrees such that the muscle fibers were parallel to the stainless steel plates and measurements repeated (transverse measurements). To ensure consistent temperature, the entire cell was maintained at 37°C through the use of a heating pad surrounding the cell. After measurements were completed, the muscle tissue was immediately frozen in isopentane cooled in liquid nitrogen for histological analysis (see below) and stored at −80°C until ready for use.

2.5 Quantitative histology

The frozen tissue was cut in a Tissue Tek II cryostat (Miles Laboratories, Inc., Elkhart, IN) into10 μm thick sections and stained with Hematoxylin and Eosin (Dubowitz 1985). The same superficial section of gastrocnemius used for the impedance measurements was used for the histological analysis. The slides were chosen blind to group, but based on their having high quality staining and good cross sectional muscle fiber orientation. Given the time-consuming nature of the histological analysis, tissue from only the last 8 consecutive healthy mature animals were used (in other words, 4 healthy mature animals' histology was not assessed, leaving all 8 animals in each of the 3 groups).

Standard stereological measurements (Mayhew *et al* 1997) were made on a Zeiss Axiophot microscope with a LUDL motorized stage interfaced with a Dell Optiflex 380 computer running Stereo Investigator (MBF Biosciences, Inc, Williston, VT) software. This software allows a non-biased quantification of fiber sizes and muscle fibers to be counted. After the investigator sets a series of initial parameters, including the section of tissue from which to choose cells, the system automatically and randomly selects groups of cells to count. A total of approximately 300 cells were evaluated from each animal. In order to further reduce the potential for any bias, the evaluator (PMF) was blinded as to the type of section (immature

animal, adult healthy animal, sciatic crush animal). For each slide, a histogram of cell size (in cross-sectional area and diameter) is obtained.

2.6 Data analysis

Calculation of electrical constants—Resistance and reactance were measured from the muscle piece in plexiglass cell. The measured complex impedance of the muscle can be written as:

$$Z=R+jX \tag{1}$$

Alternatively, the complex admittance is written as:

$$Y=\frac{1}{Z}=G+j\omega C \tag{2}$$

Where, conductance G and capacitance C can be given as:

$$G=\frac{R}{R^2+X^2} \tag{3}$$

$$C=\frac{X}{(R^2+X^2)\omega} \tag{4}$$

and $\omega = 2\pi f$. The muscle's inherent electrical properties, including its conductivity and permittivity, are related to conductance and capacitance respectively, by a geometry factor, K, of the measuring system. In this case, the measuring system is the parallel plate current electrodes with two voltage measuring needle electrodes. The conductivity, σ, is related to this geometry factor, K, as:

$$\sigma=K\cdot G \tag{5}$$

And relative permittivity, ε_r is related as:

$$\varepsilon_r=\frac{K\cdot C}{\varepsilon_o} \tag{6}$$

The geometry factor,

$$K=\frac{d}{A} \tag{7}$$

where A is the contact area of the muscle and the current electrode and d is the distance between the two needle electrodes. ε_o is the permittivity of free space, which is given by 8.85×10^{-12} F/m.

Using these equations, the conductivity and permittivity values for the section of each muscle in both the longitudinal and transverse directions was calculated. Data were plotted across the entire frequency spectrum of measurement from 2 kHz to 1 MHz, and also reported at specific frequencies of 50 kHz, 100 kHz, 500 kHz, and 1 MHz.

Correlation of impedance data to muscle histology: For each animal, the median, rather than mean muscle fiber size was measured since the distribution of fibers was sometimes skewed. Rank correlation (Spearman) was performed to relate the measured dielectric constants for muscle from each individual animal and the measured muscle fiber area. Two-group comparisons were made *via* standard t-tests as the group data were normally distributed with equal variances. Significance was kept at 0.05, two-tailed for all measurements. Statistical analyses were completed using SPSS (SPSS, Inc, Chicago, IL).

3. RESULTS

3.1 Changes in electrical constants in longitudinal and transverse directions

Figure 1 provides the average conductivity and relative permittivity data across the frequency spectrum in both the longitudinal and transverse directions for all three categories of animals: immature, mature, and sciatic crush. Tables 1 and 2 provide statistical analyses at selected frequencies of 50 kHz, 100 kHz, 500 kHz, and 1MHz for these data. Conductivity in the longitudinal direction is similar between immature and mature animals. Likewise, permittivity in the longitudinal direction is not significantly different, although it is somewhat higher in the mature rats at low frequencies and lower in the mature rats at high frequencies. However, there are significant differences at most frequencies for both the *transverse* conductivity and relative permittivity, both being higher in the mature rats as compared to the immature.

When comparing the sciatic-crush and the healthy mature animals, conductivity at all frequencies is higher in both transverse and longitudinal directions in the sciatic crush animals. Relative permittivity, although slightly higher in the crush animals at all but the lowest frequencies, is not significantly different.

In regard to our non-significant results for the comparisons between immature animals, we would expect to have a greater than 90% power to detect a 0.16 S/m difference in longitudinal conductivity and greater than 90% power to detect a difference of 1600 in longitudinal relative permittivity at 50 kHz. In regard to the non-significant comparisons between mature and crush animals, we would still have about the same power for the longitudinal conductivity measurements, but only about an 80% power to detect a difference of 12000 in the longitudinal relative permittivity at 50 kHz.

3.2 Histological differences and relation to quantified measures

Immature rats had, on average (± standard error of the mean), a median muscle fiber area of $1590 \pm 155\ \mu m^2$ (range 902–2372 μm^2) whereas mature rats had, on average, a median muscle fiber area of $3220 \pm 148\ \mu m^2$ (range 2453–3756 μm^2); the crush animals had a median area of $2082 \pm 60 \mu m^2$ (range 1967–2457 μm^2). The differences between mature and immature, and between mature and crush, were significant ($p < 0.001$ for both comparisons). Examples of pathology are presented in Figure 2 which shows prototypical data from an immature animal, a mature animal and a mature animal within 2 weeks of crush injury. Figure 3 shows scatter plots relating the different groups of animals to their muscle fiber areas.

With growth from immaturity to maturity, the major changes observed are in the transverse measurements: both relative permittivity and conductivity increase linearly with muscle fiber area. Indeed, linear regression of all the non-crush animals (mature and immature) shows a

strong relation (Spearman's rho = 0.879 ($p < 0.001$) for transverse conductivity and muscle fiber area and Spearman's rho = 0.865 ($p < 0.001$) for transverse permittivity). In comparison neither longitudinal parameter shows substantial variation in muscle fiber size in health (Spearman's rho= −0.129, NS for conductivity and 0.198, NS for permittivity).

With crush, the major change is an increase in longitudinal conductivity as noted above and less so in transverse conductivity with no substantial change in the relative permittivity in either direction. It is worthwhile to highlight that although the muscle cells after crush are more comparable in size to those of the immature animals, they have a higher rather than a lower transverse conductivity and relative permittivity (see Figure 3b and 3d)

4. DISCUSSION

The data presented here confirm that significant changes to the electrical properties of skeletal muscle occur with rat growth and within 1–2 weeks after sciatic nerve injury. Indeed, our data for mature rat muscle corresponds well for values in rats and in other species as reported in a comprehensive review of the literature (Gabriel *et al* 1996). However, data on immature rats and on rat muscle after nerve injury have not been previously reported.

The changes in the electrical constants with animal growth likely reflect changes in the size of the myocytes, which is confirmed on our quantitative histological analysis and the remarkably strong linear relation between muscle fiber size and measured transverse conductivity and relative permittivity. Increasing membrane area likely makes the muscle more easily polarized thus leading to an increase in its relative permittivity. However, these changes may reflect more than just enlargement in the myocytes themselves, as the interstitium of the muscle also undoubtedly undergoes modification with growth. Other non-muscular factors could also play a role, including, for example, a maturing muscle vascular supply.

After sciatic nerve crush, there are very clear changes in the conductivity of the tissue, more so in the longitudinal than in the transverse direction, and non-significant changes in the relative permittivity. These changes may parallel those changes in the T2 signal observed on magnetic resonance imaging (MRI) of muscle after nerve injury (Wessig *et al* 2004; Polak *et al* 1988). There are two explanations offered for these T2 changes: (1) that caused by an increase in the extracellular space (Polak *et al* 1988)or (2) an increase in the size of the capillary bed (Wessig *et al* 2004). However, in the case of electrical impedance measurements, in addition to these two possibilities, changes in the membrane polarity or channel function could also play important roles.

Given that much of our clinical work is focused on measuring the surface impedance properties of muscle in diseased states, we are also quite interested in understanding how the changes observed here relate to surface values. With surface measurements, we have generally observed reductions in the phase angle due to a simultaneous elevation in the resistance and a reduction in reactance of the tissue in diseased states (Rutkove *et al* 2002; Tarulli *et al* 2005; Rutkove *et al* 2007). However, the increasing conductivity of muscle we observed here would be expected to produce a *reduction* in the measured surface resistance. Thus, the observed elevations in surface resistance are most likely a simple volumetric effect: a reduced area through which current can travel will increase the measured resistance. Although, presumably, the increased conductivity will offset this to some extent, it is insufficient. Similarly, the lack of any substantial change in the relative permittivity at 50 kHz in this study points to the likelihood that the observed effects are mostly volumetric in nature also, as clear reductions in the reactance are also generally observed in disease states.

A similar volumetric argument can be made for our surface data on immature animals in which we have also observed resistance being slightly higher in the younger animals and gradually

decreasing and stabilizing as the animal reaches maturity (at about 350gms)(Ahad and Rutkove 2009). However, the same volumetric explanation cannot explain the elevated reactance of immature animals. Indeed, elevation in measured surface reactance is consistent with the reduced relative permittivity of the tissue in the immature animals measured here.

Although these data suggest that single-frequency surface impedance measurements are, for the most part, mainly providing a means for assessing muscle volume in nerve injury and with animal growth, the same may not be true for the behavior of the overall frequency spectrum. Indeed, the marked elevations in reactance values at high frequencies in patients with chronic neuromuscular disease (Esper *et al* 2006) suggest that the complexities of the frequency spectrum will reveal additional insights into tissue characteristics beyond simple volumetric change. The complexity of these frequency dependent changes is hinted at in Figure 1 as the curves for the different groups of animals do not simply parallel each other. However, a full analysis of these frequency dependencies is beyond the scope of this study.

There are several limitations to this work worth highlighting. First, variability in the severity of the experimental crush lesion undoubtedly contributed to some of the variability in the observed measurements of the electrical constants. Second, although we attempted to perform these measurements as expeditiously as possible after each animal was killed, it is essentially impossible to know what these measurements would have shown if the muscle fibers were actually alive at the time of measurement. Accordingly, some caution most be exercised when comparing these values to those obtained with surface measurements on a living animal. Third, we are dealing with relatively small sizes of tissue in the normal rat and these tissue sizes become even smaller when the rats are immature or there is crush injury. Since the calculation of these constants requires a careful size measurement of the muscle, this undoubtedly also contributes to some of the observed variation. Fourth, even modest variations in the moistness of the tissue may contribute noise. We attempted to assure all samples were treated identically, but this too is clearly subject to some variation. Finally, some variation in the size of the muscle fibers due to shrinkage artifact may also have occurred due to our inability to pin or otherwise secure the tissue immediately after its removal from the animal; however, no obvious shrinkage was observed on histological analysis.

The main focus of this work was the correlation of muscle fiber electrical properties to muscle fiber size. We specifically did not attempt to evaluate fiber type distributions or attempt to correlate these distributions to the changes in conductivity or relative permittivity. Although a potentially important question, as it is unknown whether fiber type actually impacts the electrical conductivity and permittivity of individual muscle fibers, pursuing that question as part of this study would have not been ideal. In order to answer this question most effectively, a study correlating the electrical properties of multiple muscles with different fiber type proportions in a group of adult healthy rats would be far more informative since muscle fiber size could be kept constant. Second, we were interested in evaluating acute changes in the muscle after nerve injury, and over the short time period evaluated here, limited reinnervation of the gastrocnemius muscle would have occurred and thus limited or inconsistent changes in fiber type would be expected, making the results of such an analysis even more uncertain. Nonetheless, this remains a very important question and will be pursued separately as part of our future planned work.

In addition to these limitations, the relevance of these initial rat-based studies to our human data needs to be considered. While the changes do mimic human nerve injury, much of our human studies, by necessity, have been in individuals with chronic not acute or subacute injuries. For example, we have reported findings in patients with chronic radiculopathy, amyotrophic lateral sclerosis, and polio (Rutkove *et al* 2002; Rutkove *et al* 2005; Rutkove *et al* 2007). Thus, in order to specifically address this question, it will be necessary to study the

time course of changes over a several month period. It is very possible that the early elevations in conductivity seen here might reverse as the muscle develops increased interstitial fat and connective tissue with loss of free water.

In summary, we have shown that muscle's inherent conductivity and relative permittivity change with growth and after sciatic nerve crush. In order to more fully apply impedance methods to neuromuscular disease states, it will be necessary to build upon the basic foundation laid out here by studying additional disease models, including models of disuse atrophy, muscular dystrophy, toxic myopathy, and neurodegenerative diseases, including ALS. We also plan to incorporate the data obtained here into finite element models to better understand how the muscle's electrical properties relate to the observed surface measurements. For example, using the results of this work, it may be possible to more effectively interpret surface impedance data for diagnostic purposes. Alternatively, it may provide a new approach for muscle tissue evaluation by assessing its electrical properties in addition to its pathology.

5. Conclusion

We have studied the electrical properties of skeletal muscle in immature rats, mature rats, and mature rats after sciatic nerve injury and have correlated these values with muscle fiber diameter. Both transverse conductivity and relative permittivity increase with increasing muscle fiber diameter in healthy rats. Sciatic crush has minimal effect on the relative permittivity of the tissue, but increases its conductivity in both orientations significantly. The frequency dependence of these values also changes with growth and after nerve injury.

Acknowledgments

The authors thank Professors Carl Shiffman and Ronald Aaron of Northeastern University for their support and for the development of the system used to make these measurements. This study was funded by the National Institutes of Health Grant RO1-NS055099.

References

Ahad M, Rutkove SB. Electrical impedance myography at 50 kHz in the rat: technique, reproducibility, and the effects of sciatic injury and recovery Clinical Neurophysiology. Clinical Neurophys. 2009 June 29; (epub).

Baumann SB, Wozny DR, Kelly SK, Meno FM. The electrical conductivity of human cerebrospinal fluid at body temperature. IEEE Trans Biomed Eng 1997;44:220–3. [PubMed: 9216137]

Epstein BR, Foster KR. Anisotropy in the dielectric properties of skeletal muscle. Med Biol Eng Comput 1983;21:51–5. [PubMed: 6865513]

Dubowtiz, V. Muscle biopsy: a practical approach. 2. Balliere Tindal; Philadephelia: 1985. p. 29

Esper, GJ.; Shiffman, CA.; Aaron, R.; Lee, KS.; Rutkove, SB. Muscle Nerve. Vol. 34. 2006. Assessing neuromuscular disease with multifrequency electrical impedance myography; p. 595-602.

Gabriel C, Gabriel S, Corthout E. The dielectric properties of biological tissues: I. Literature survey. Phys Med Biol 1996;41:2231–49. [PubMed: 8938024]

Garmirian LP, Chin AB, Rutkove SB. Discriminating neurogenic from myopathic disease via measurement of muscle anisotropy. Muscle Nerve 2009;39:16–24. [PubMed: 19058193]

Mayhew TM, Pharaoh A, Austin A, Fagan DG. Stereological estimates of nuclear number in human ventricular cardiomyocytes before and after birth obtained using physical disectors. J Anat 1997;191 (Pt 1):107–15. [PubMed: 9279664]

Nie R, Chin AB, Lee KS, Sunmonu NA, Rutkove SB. Electrical impedance myography: transitioning from human to animal studies. Clin Neurophys 2006;117:1844–9.

Polak JF, Jolesz FA, Adams DF. Magnetic resonance imaging of skeletal muscle. Prolongation of T1 and T2 subsequent to denervation. Invest Radiol 1988;23:365–9. [PubMed: 3384617]

Rutkove SB, Zhang H, Schoenfeld DA, Raynor EM, Shefner JM, Cudkowicz ME, Chin AB, Aaron R, Shiffman CA. Electrical impedance myography to assess outcome in amyotrophic lateral sclerosis clinical trials. Clin Neurophysiol 2007;118:2413–8. [PubMed: 17897874]

Rutkove SB. Electrical Impedance Myography: Background, Current State, and Future Directions. Muscle Nerve. 2009 (in press).

Rutkove SB, Aaron R, Shiffman CA. Localized bioimpedance analysis in the evaluation of neuromuscular disease. Muscle Nerve 2002;25:390–7. [PubMed: 11870716]

Rutkove SB, Esper GJ, Lee KS, Aaron R, Shiffman CA. Electrical impedance myography in the detection of radiculopathy. Muscle Nerve 2005;32:335–341. [PubMed: 15948202]

Tarulli A, Esper GJ, Lee KS, Aaron R, Shiffman CA, Rutkove SB. Electrical impedance myography in the bedside assessment of inflammatory myopathy. Neurology 2005;65:451–452. [PubMed: 16087913]

Wessig C, Koltzenburg M, Reiners K, Solymosi L, Bendszus M. Muscle magnetic resonance imaging of denervation and reinnervation: correlation with electrophysiology and histology. Exp Neurol 2004;185:254–61. [PubMed: 14736506]

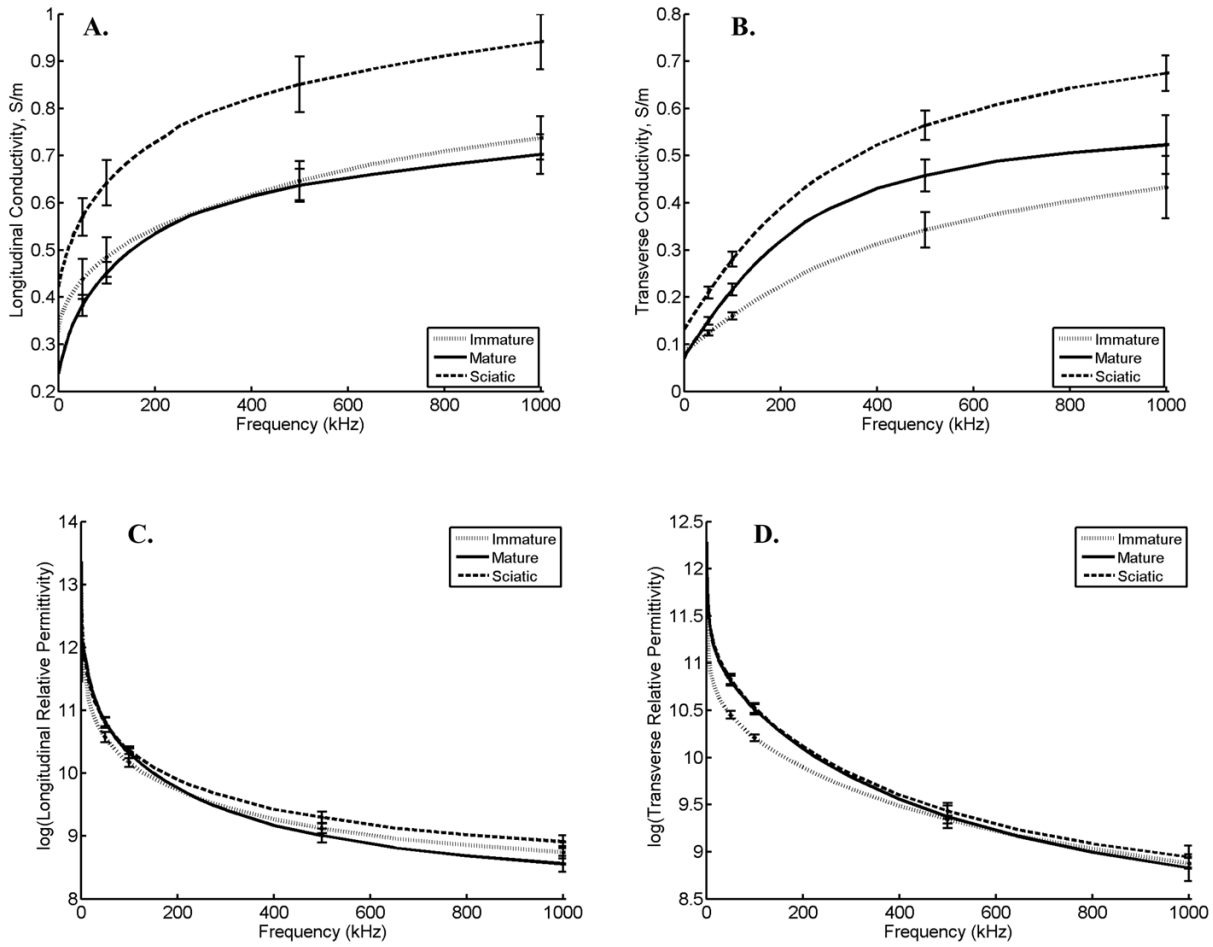

Figure 1.

Conductivity and permittivity values (± standard error at selected frequencies) for the 3 groups of animals (immature, mature, and sciatic crush). **A.** Longitudinal conductivity from 2kHz to 1MHz. **B.** Transverse conductivity from 2 kHz to 1 MHz (note the different scales between 1A and 1B). **C.** Log(Longitudinal permittivity) from 2kHz to 1MHz. **D.** Log(Transverse permittivity) from 2 kHz to 1MHz

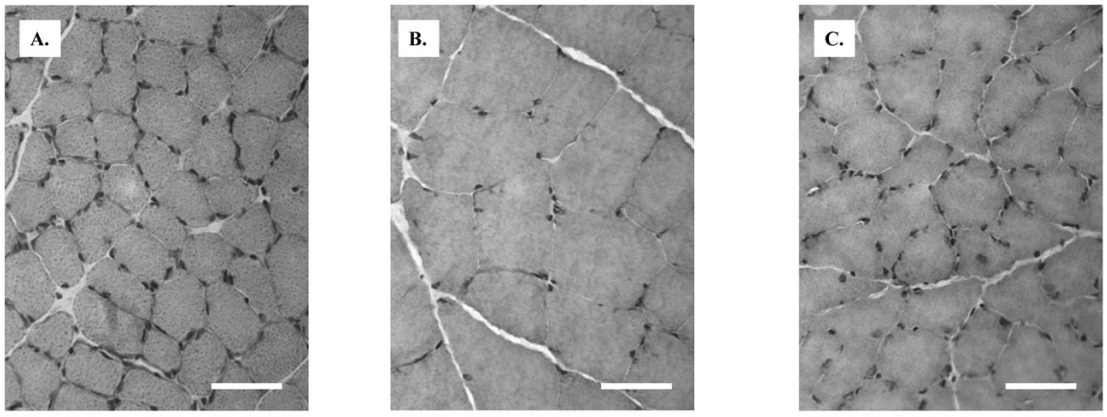

Figure 2.

A. Gastrocnemius muscle from immature rat (40X), Hematoxylin and Eosin. **B.** Gastrocnemius muscle from mature rat (40X), Hematoxylin and Eosin **C.** Gastrocnemius muscle from mature rat 2 weeks after sciatic crush (40X), Hematoxylin and Eosin. Bar = 50 μm

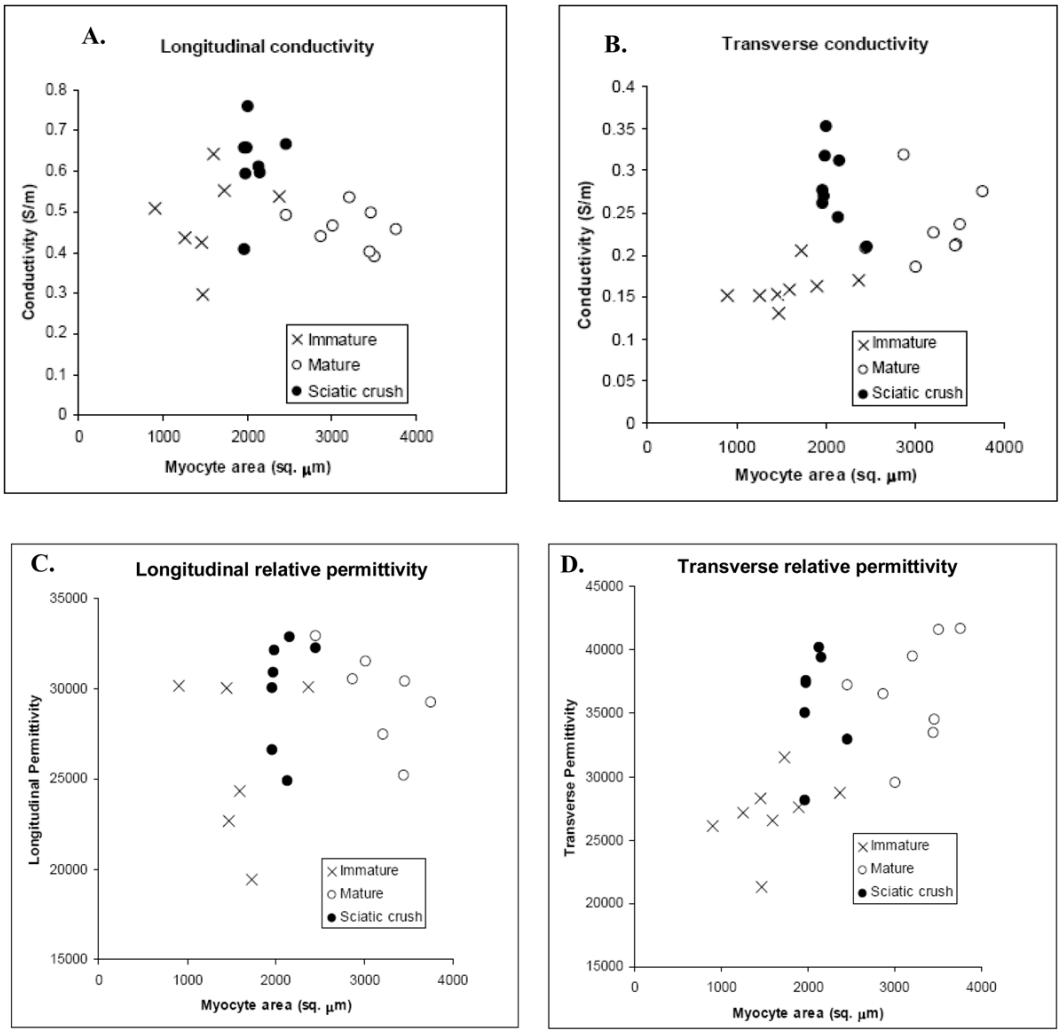

Figure 3.

Scatterplots comparing the four electrical parameters to myocyte size. Each point represents the value from an individual animal. Note the prominent near-linear relation between transverse measurements and myocyte size in the immature and mature healthy animals and the lack of a relation in the longitudinal direction. In addition, crush animals show an elevation in conductivity in both longitudinal and transverse directions.

Table 1

Longitudinal and transverse conductivities (S/m) and permittivities (± standard error of the mean) of immature and mature rat gastrocnemius muscle

Frequency	**50kHz**		**100kHz**		**500kHz**		**1MHz**	
Conductivity (S/m)	σ_L	σ_T	σ_L	σ_T	σ_L	σ_T	σ_L	σ_T
Immature (N=8)	0.44±0.04	0.12±0.01	0.49±0.03	0.16±0.01	0.65±0.04	0.34±0.04	0.74±0.05	0.43±0.07
Mature (N=12)	0.38±0.02	0.15±0.01	0.45±0.02	0.22±0.01	0.64±0.04	0.46±0.03	0.70±0.04	0.52±0.06
Significance	ns	**0.03**	ns	**0.002**	ns	**0.05**	ns	ns
Permittivity	ε_L	ε_T	ε_L	ε_T	ε_L	ε_T	ε_L	ε_T
Immature (N=8)	39100±3200	34600±1400	26100±1900	27200±1000	9100±760	11400±460	6300±650	7200±400
Mature (N=12)	47400±3100	47600±1900	29200±2200	35100±1400	8400±900	11400±1000	5300±600	7000±1100
Significance	ns	**0.001**	ns	**0.002**	ns	ns	ns	**0.04**

σ_L, longitudinal conductivity; **σ_T,** transverse conductivity; **ε_L,** longitudinal permittivity; **ε_T,** transverse permittivity

Table 2

Longitudinal and transverse conductivities (S/m) and permittivities (± standard error of the mean) of rat gastrocnemius muscle of healthy mature rats and rats within 2 weeks of sciatic nerve crush.

Frequency	**50kHz**		**100kHz**		**500kHz**		**1MHz**	
Conductivity(S/m)	σ_L	σ_T	σ_L	σ_T	σ_L	σ_T	σ_L	σ_T
Mature (N=12)	0.38±0.02	0.15±0.01	0.45±0.02	0.22±0.01	0.64±0.04	0.46±0.03	0.70±0.04	0.52±0.06
Sciatic Crush (N = 8)	0.55±0.03	0.21±0.01	0.62±0.04	0.28±0.02	0.82±0.04	0.56±0.03	0.91±0.04	0.67±0.04
Significance	**0.004**	**0.002**	**0.009**	**0.006**	**0.004**	**0.02**	**0.007**	**0.04**
Permittivity	ε_L	ε_T	ε_L	ε_T	ε_L	ε_T	ε_L	ε_T
Mature (N=12)	47400±3100	47600±1900	29200±2200	35100±1400	8400±900	11400±1000	5300±600	7000±1100
Sciatic Crush (N = 8)	45800±2700	48500±2000	29900±1100	35800±1500	10500±1000	12200±1200	7100±800	7600±1000
Significance	ns	ns	ns	ns	ns	ns	ns	ns

σ_L, longitudinal conductivity; **σ_T,** transverse conductivity; **ε_L,** longitudinal permittivity; **ε_T,** transverse permittivity